J Solid State Electrochem (2015) 19:1427–1435
DOI 10.1007/s10008-015-2762-6

ORIGINAL PAPER

Modified TiO_2-SiO_2 ceramic filler for a composite gel polymer electrolytes working with $LiMn_2O_4$

Beata Kurc · Teofil Jesionowski

Received: 27 November 2014 / Revised: 13 January 2015 / Accepted: 18 January 2015 / Published online: 31 January 2015
© Springer-Verlag Berlin Heidelberg 2015

Abstract A new type of ceramic filler (TiO_2-SiO_2) was used in composite gel polymer electrolytes for application in lithium-ion batteries ($LiMn_2O_4$|Li). TiO_2-SiO_2 ceramic powders were obtained by co-precipitation from solutions of titanium sulphate and sodium silicate. The resulting submicron-size powders were used as fillers in composite gel polymer electrolytes for Li-ion batteries based on polyacrylonitrile (PAN) membranes and sulpholane (TMS). The composite gel polymer electrolytes (PE) were analysed structurally and electrochemically, demonstrating favourable properties in terms of electrolyte uptake and electrochemical characteristics in Li-ion cells. The surface morphology of the PE was studied using scanning electron microscopy (SEM). It was found to be a stable, porous and flexible polymer electrolyte with an ionic conductivity of 9.8×10^{-4} S cm^{-1} at 25 °C. The performance of the $LiMn_2O_4$|PE3|Li cell was tested using electrochemical impedance spectroscopy (EIS) and galvanostatic charge/discharge. The $LiMn_2O_4$ cathode exhibited good cyclability and coulombic efficiency (ca. 145 mAh g^{-1} after 50 cycles) when used together with 1 M $LiPF_6$ in PAN/TMS/TiO_2-SiO_2+ 8 wt.% VC.

Introduction

Composite polymer electrolytes (CPEs) have received extensive attention in recent decades for their potential application in higher-energy-density and higher-power-density lithium batteries, owing to their lack of leakage, high flexibility within the cell geometry, high physical and chemical stability and good interfacial compatibility with electrodes [1–5]. One of the most promising ways to obtain CPEs is the addition of nanosized or microsized ceramic fillers. The positive effect of various ceramic particles (SiO_2 [3, 6], Al_2O_3 [4] and TiO_2 [5, 7, 8]) on the conductivities of dry polymer electrolytes is also well documented in the literature.

The obtained CPEs alone can offer improved ionic conductivity, mechanical strength and electrolyte-electrode compatibility. Generally speaking, a CPE used as a device component must be capable of maintaining its rated performance for a sufficiently long time, as appropriate to the particular application [9, 10].

Increased interest in inorganic oxide systems has prompted the intensive development of methods for their synthesis and functionalisation. This interest stems from their specific physicochemical properties such as large surface area and chemical and thermal stability, which are vital for the production of composite systems, such as TiO_2-SiO_2 composite materials [11–16]. Specific applications of such oxide systems or their derivatives require well-defined physicochemical parameters [17–19]. The physicochemical properties of the functionalised commercial and synthetic oxide systems depend mainly on the effectiveness of the modification process and its implementation [20, 21]. The effectiveness of inorganic oxide systems' surface functionalisation is evaluated on the basis of adsorption properties, dispersion and morphological characterisation, hydrophobic/hydrophilic properties and chemical interactions, as well as electrokinetic measurements [17–24].

A combination of TiO_2 with crystalline structure and SiO_2 with amorphous structure permits the majority of the aforementioned desired properties to be attained. The presence of SiO_2 brings a reduction in the particle size and an increase in the surface area or in the mechanical strength [25–27]. The

B. Kurc (✉)
Institute of Chemistry and Electrochemistry, Faculty of Chemical Technology, Poznan University of Technology, Berdychowo 4, 60965 Poznan, Poland
e-mail: beata.kurc@put.poznan.pl

T. Jesionowski
Institute of Chemical Technology and Engineering, Faculty of Chemical Technology, Poznan University of Technology, Berdychowo 4, 60965 Poznan, Poland

composite is chemically neutral and UV-transparent and has a large surface area [28]. The presence of SiO_2 is also responsible for the increased thermal stability of the composite, which prevents transformation of anatase TiO_2 into its rutile variety [25]; this is of profound importance, as anatase has the highest photocatalytic activity of all three varieties [26]. TiO_2-SiO_2 oxide composites are used as effective catalysts and photocatalysts for, for example, the polycondensation of poly(ethylene terephthalate), hydration of carbon oxide or selective oxidation by peroxides of organic compounds in the liquid phase. TiO_2-SiO_2 oxide composite also acts as a photocatalyst in the neutralisation of wastewater from the production of nitriles, nylon, plastics, synthetic rubber, benzene, nitrobenzene, herbicides and gold [26, 27].

Incorporation of an inorganic filler into the gel polymer electrolyte further increases the uptake of the liquid electrolyte and enhances the dimensional stability of the membrane [28–31]. These advantages have inspired extensive research into the use of gel polymer electrolyte and composite gel polymer electrolytes in lithium/sulphur (Li/S) batteries [32–41].

It was decided to use a new polymer electrolyte to investigate the system $LiMn_2O_4$|PE3|Li (Table 1).

$LiMn_2O_4$ is ideal as a high-capacity Li-ion battery cathode material by virtue of its low toxicity, low cost and the high natural abundance of Mn. A further advantage of spinel is its high thermal stability and enhanced safety; however, the cycle life and calendar life are limited. Low internal cell resistance is the key factor for fast charging and high-current discharging. This spinel structure, which is usually composed of diamond shapes connected into a lattice, appears after initial formation. Spinel provides low resistance but has a more moderate specific energy than cobalt. Li-manganese has a capacity lower by roughly one-third than that of Li-cobalt, but the battery still offers about 50 % more energy than nickel-based chemistries. Design flexibility allows engineers to optimise the battery for either longevity (life span), maximum load current (specific power) or high capacity (specific energy). For example, the long-life version in the 18650 cell has a moderate capacity of 1100 mAh; the high-capacity version provides 1500 mAh but has a reduced life span.

Spinel-type lithium-manganese oxide $LiMn_2O_4$ is one of the most frequently studied cathode materials for use in Li-ion batteries. It has a specific capacity of 120 mAh g^{-1} between 3.5 and 4.3 V and has no memory effects [42, 43]. However, the theoretical capacity of the spinel is 148 mAh g^{-1} [44]. In addition, $LiMn_2O_4$ is cheap and contains no heavy metals; hence, it is environmentally friendly. $LiMn_2O_4$ has been examined in ionic liquids based on trimethylhexylammonium [45, 46], N-methyl-N-propylpiperidinium [47], 1-cyanomethyl-3-methylimidazolium [48] cations and bis(trifluoromethanesulphonyl)imide anion. The $LiMn_2O_4$ cathode in the ionic liquid was observed to exhibit thermal stability, which is a favourable property for the improvement of battery cell safety. The phosphazenic compound triethoxyphosphazen-N-phosphoryldiethylester [49] and a binary mixture of triethylphosphate and EC [47] have also been studied as non-flammable electrolyte additives for Li-ion cells with the $LiMn_2O_4$ cathode [50].

The role of the two oxides in industry is therefore enormous. However, titania's high tendency towards agglomeration has prompted scientists to search for ways to limit this phenomenon. The addition of silica can improve the degree of dispersion of titania as well as increasing its activity and contributes to the transformation of anatase into the rutile form. There are many methods for preparing hybrid TiO_2-SiO_2 oxide, which lead to products with different properties. It may be expected that certain favourable properties of both SiO_2 and TiO_2 will be reinforced and a synergic effect will be detected.

Thus, the motivation of this work was to examine the properties of a hybrid TiO_2-SiO_2 filler for CPEs.

In this study, a $LiMn_2O_4$ lithium-polymer battery, comprising a PAN/TMS/TiO_2-SiO_2 composite polymer membrane, was assembled and examined. The electrochemical performance of the $LiMn_2O_4$|PE3|Li polymer battery was examined using a galvanostatic charge-discharge method at variable rates.

Table 1 Polymer electrolyte composition and specific conductivity of the gel at 25 °C

Electrolyte	Composition/wt%				Specific conductivity/ S cm^{-1}
	PAN	TMS	$LiPF_6$	TiO_2-SiO_2	
PE3	20.15	70.70	6.15	3	9.8×10^{-4}

Experimental

Materials

The composite material was precipitated by an emulsion system with the use of cyclohexane (POCh SA, analytical grade) as the organic phase. The procedure is described in detail in a previous publication [51].

$LiMn_2O_4$ powder (Aldrich), graphite KS-15 (G) (Lonza), poly(vinylidene fluoride) (PVdF, MW=180,000 Fluka), lithium foil (Aldrich, 0.75 mm thick), vinylene carbonate (VC, Aldrich), N-methyl-2-pyrrolidinone (NMP, Fluka), polyacrylonitrile (PAN, Aldrich), dimethylformamide (DMF, Aldrich), lithium hexafluorophosphate ($LiPF_6$, Aldrich) and sulpholane (TMS, Fluka) were used as received.

Preparation of titania/silica support

A detailed description of the TiO_2-SiO_2 oxide composite emulsion-precipitation process has appeared in previously published work (Scheme 1) [51].

Preparation of the polymer and electrode

Composite gel polymer electrolytes (PEs) were prepared by the casting technique. First, the polymer (PAN) was swollen in DMF at 60 °C. After 24 h, the polymer solution was mixed with the electrolyte (1 M $LiPF_6$ in TMS), both pure and with the addition of 3 wt.% TiO_2-SiO_2. The viscous solution of the polymer in a mixture of the solvent (DMF) and sulpholane was cast onto a glass plate. Sulpholane was the environment used to dissolve the salt $LiPF_6$. Moreover, sulpholane (TMS) plays the role of both plasticiser and diluent of the lithium salts or ionic liquid, which makes the system more conductive. After weighing, the plate was transferred to a desiccator, where the solvent was slowly evaporated under a stream of dry nitrogen, first at room temperature, then at 60 °C and finally at reduced pressure.

After evaporation of the volatile component, the plate with the composite gel polymer electrolyte foil was reweighed, and the composition was determined from the mass balance (with an accuracy of 10^{-4} g). When the appropriate weight of non-volatile components was attained, this suggested that all of the DMF had been removed. The thickness of the electrolytes was in the range 0.2–0.4 mm. All samples were prepared in a glove box in an argon atmosphere.

The composition of the final composite gel polymer electrolyte is given in Table 1. The resulting gel-type polymer electrolytes were free-standing, homogeneous membranes. The polymer electrolyte was soaked with a drop of vinylene carbonate (VC, 7–8 %) before the cells were assembled. Generally, the electrochemical reaction of the electrolyte additive (for example, lithium carbonate or salicyloborate, vinylene carbonate, etc.) at the graphite electrode may result in the formation of a coating and modification of the electrode surface. Vinylene carbonate seems to be one of the most effective additives to the electrolyte. Positive electrodes were prepared by casting a slurry of the $LiMn_2O_4$, graphite (G) and PVdF (in the ratio 85:5:10) in N-methyl-2-pyrrolidone (NMP, Fluka) on a gold current collector (anticorrosive, radius 12 mm). The cathode layer was formed by vacuum evaporation of the solvent (NMP) at 120 °C. The electrode typically contained 1.5–2.5 mg of $LiMn_2O_4$.

Tested anodes were prepared on a copper foil (Hohsen, Japan) by the casting technique, from a slurry of graphite (G), carbon black (CB) and PVdF in NMP. The ratio of components was G/CB/PVdF=85:5:10 (by weight). After evaporation of the solvent (NMP) at 120 °C in vacuum, a layer

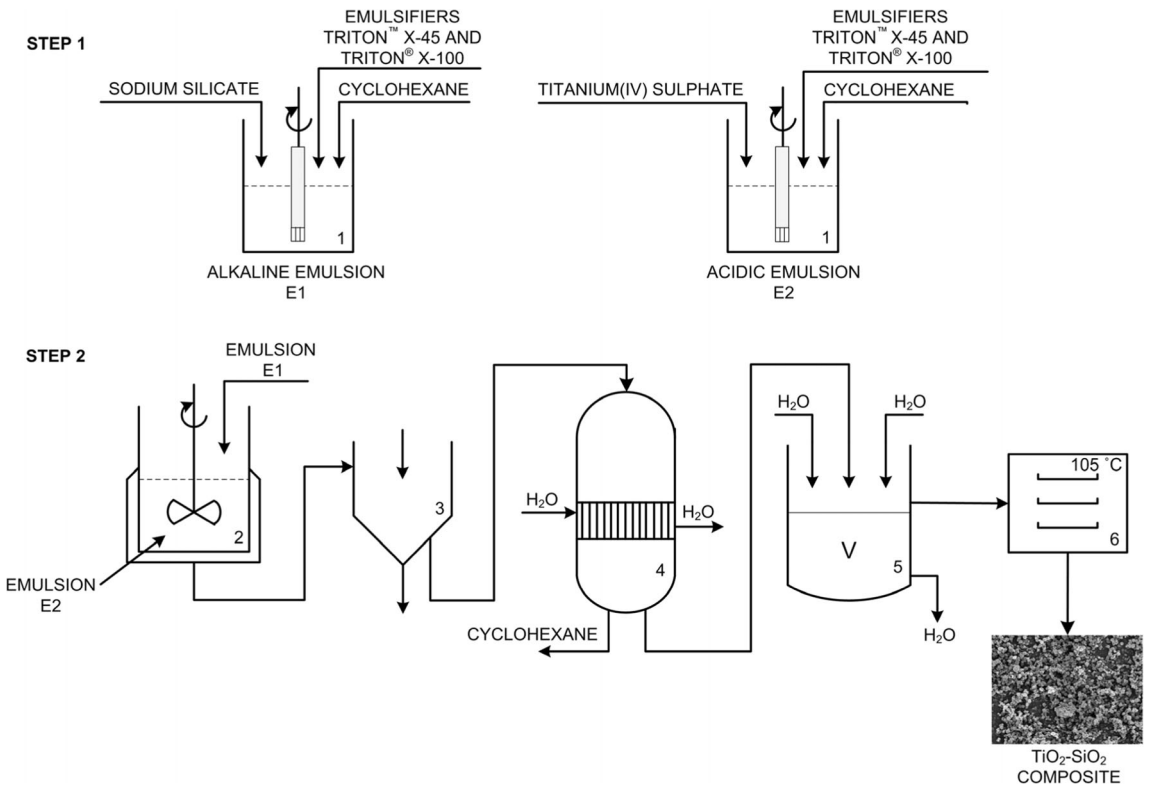

Scheme 1 Technological scheme of TiO_2-SiO_2 ceramic filler using emulsion-precipitation method: *1* open container, *2* reactor with stirrer, *3* decanter, *4* vacuum evaporator, *5* vacuum filter, *6* stationary drier

containing the active material (G), the electronic conductor (CB) and the binder (PVdF) was formed on the carbon electrode. Typically, the masses of the electrodes were as follows: Li: ca. 45 mg (0.785 cm^2); anode: 3.0–4.0 mg.

Measurements

Electrochemical properties of the cells were determined using electrochemical impedance spectroscopy (EIS) and galvanostatic charging/discharging tests. The $LiMn_2O_4$|PE3|Li cells were assembled in a dry argon atmosphere in a glove box. Lithium foil and a cathode electrode were separated by the polymer electrolyte, placed in an adapted Swagelok® connecting tube. The geometrical surface area of the Li and $LiMn_2O_4$ electrodes was 1 cm^2. Interface resistance at the electrode/polymer electrolyte interface was measured with an AC impedance analyser (Atlas-Sollich Systems, Poland). The impedance spectra were recorded from 0.01 Hz to 10 kHz at an amplitude of 10 mV.

The conductivity of the electrolytes was measured in a two-electrode (Pt) thermostated conductometric glass cell with a constant of 4.80 cm^{-1}. The corresponding conductivity data for polymer electrolytes, sandwiched between two gold blocking electrodes, were measured in the Swagelok® connecting tube, placed in an air thermostat. In the conductivity measurements of polymer electrolytes, impedance values were recorded between 1 Hz and 10 kHz at an amplitude of 10 mV.

The morphology of the polymer electrolyte was observed with a scanning electron microscope (SEM, Tescan Vega 5153).

Results and discussion

A high ionic conductivity (1.47×10^{-3} S cm^{-1}) was determined for a PAN-PVA/EC/DMC/$LiBF_4$ system with molar ratio 20:28:45:7. The charge/discharge performance of the maximum ionic conductivity complex was also studied. The practical performance and thermal stability of Li-ion polymer batteries with $LiNi_{0.8}Co_{0.2}O_2$, mesocarbon microbead-based graphite and poly(acrylonitrile) (PAN)-based gel electrolytes were reported by Akashi et al. [52].

Following preliminary studies using composite gel polymer electrolytes based on TMS/PAN/TiO_2-SiO_2, it was decided to choose the electrolyte PE3 (see Table 1), because this exhibited the best properties and performance when used in a G|PE3|Li cell [51].

In the preparation of a polymer electrolyte using the new composite, an emulsion precipitation method was applied. The basic physicochemical properties of TiO_2-SiO_2 have been described in previous work [51], and only some of them will be highlighted here.

The essential aspect of the study was the addition of the composite functionalised with 10 % U-611 filler, in a quantity of 3 %, to the polymer electrolyte prepared based on the solution of sulpholane with $LiPF_6$ (Table 1).

Figure 1 shows the variation in ionic conductivity for PE3 over the temperature range 5–60 °C. As the graph shows, the PE3 conductivity is 9.8×10^{-4} S cm^{-1} at 25 °C and increases with temperature up to 1.5×10^{-3} S cm^{-1} at 60 °C. These results are comparable with literature data [53–56]. The conductivity of PE3 is lower than the conductivity of Li–IL solution, but this is not the most important parameter demonstrating the usefulness of an electrolyte for application in LIBs.

The conductivity data are in good agreement with solvent uptake results. Gels containing functionalised fillers exhibit the highest conductivities, approaching $\times10^{-4}$ S cm^{-1}. It is noteworthy that the highest conductivities were measured for gels with moderately functionalised fillers. Gels without any filler exhibit somewhat lower conductivity (2.0×10^{-4} S cm^{-1}) [51]. Interestingly, higher conductivity values were obtained for membranes containing sub-micro- rather than nano-sized TiO_2-SiO_2.

The morphology of a typical gel-type foil with functionalised fillers (PE3), 0.37 mm in thickness, is shown by the SEM images in Fig. 2a, b. The surface of the membrane shows the porous structure of the system. As can be seen, a porous membrane with small and uniformly distributed pores was obtained, which would improve the electrolyte solution uptake and promote stability of the GPE morphology during cycling. Moreover, small and uniformly distributed pores might increase the mechanical stability of the polymer electrolyte.

The cathode was tested in a $LiMn_2O_4$|PE3|Li cell (an example is shown in Figs. 3, 4 and 5). In all experiments, the mass of the metallic lithium counter-electrode (ca. 40 mg) was much higher than that of the tested cathode (ca. 3 mg). Figures 3 and 4 show the charging/discharging curves for the $LiMn_2O_4$|PE3|Li cell assembled from the $LiMn_2O_4$

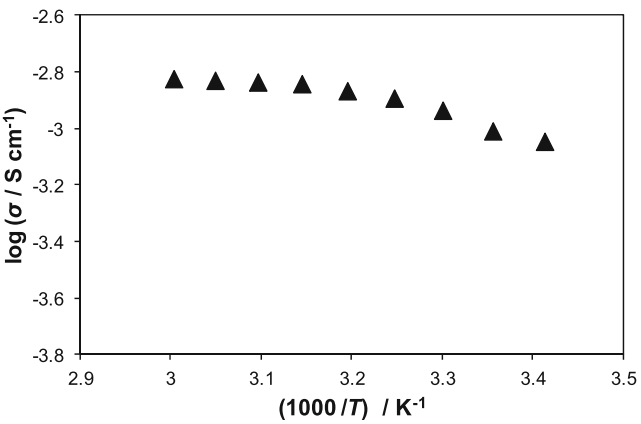

Fig. 1 The dependence of ionic conductivity on temperature for PAN/TMS/$LiPF_6$/TiO_2-SiO_2+3 *w/w* of U-611 (PE3)

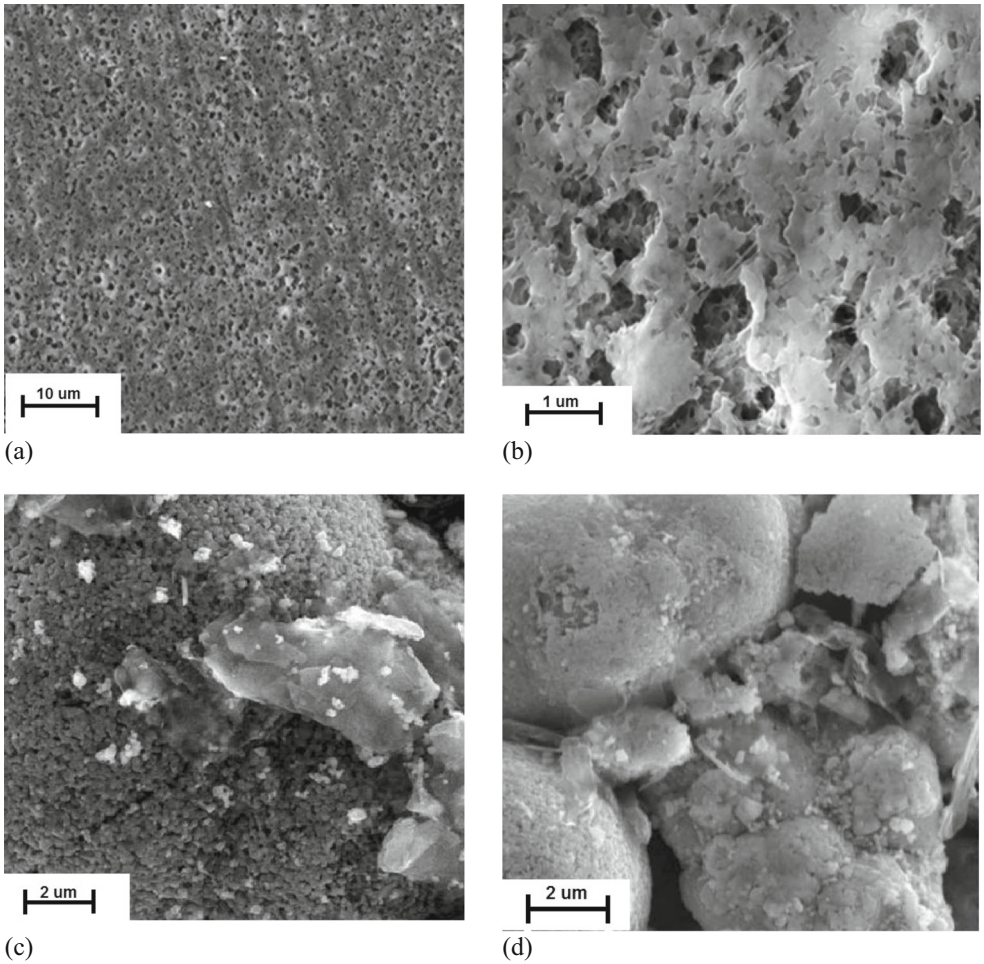

Fig. 2 SEM image of (**a, b**), PE3, (**c**) the $LiMn_2O_4$ cathode-pristine electrode and (**d**) after 30 charge/discharge cycles

cathode. It can be seen that the capacity of this electrode was stable during the cycles for all current rates.

Lithium intercalation/deintercalation in cathodic half-cells with $LiMn_2O_4$ working electrodes can be regarded as the ultimate performance test of a gel electrolyte.

Figure 3 shows the charging/discharging curve for the $LiMn_2O_4$|PE3|Li cell for different current rates. The capacities of the charging (q_{ch}) and discharging (q_{dis}) processes in the first cycle were 130 (C/5) and 160 mAh g^{-1} (C/10), respectively. As a result, the initial coulombic efficiency in the first cycle was ca. 90 and 78 %. Figure 4 shows that discharge and charge capacity increased as the current rates were varied from C/2 to C/10. Moreover, the capacities of the electrode, both q_{ch} and q_{dis}, gradually stabilised during the cycling. However, the coulombic efficiency, proportional to the ratio q_{dis}/q_{ch}, increased during the cycling, reaching almost 100 % (for C/2 and C/5) after the fourth cycle (Fig. 4). The addition of VC (8 wt.%) considerably improved both the charging and discharging capacities, in comparison with the ionic liquid without any additive (discharge capacity and coulombic efficiency for the spinel electrode used with the neat electrolyte, as well as with additive, are shown in Fig. 6). The improvement is probably due to the ability of the additive to induce solid electrolyte interface (SEI) formation on the lithium surface.

Figure 2c, d shows SEM images of a pristine electrode and those after electrochemical cycling with different electrolytes. The pristine cathode (Fig. 2c) has a morphology with an agglomerated structure and is porous. However, after electrochemical cycling in 1 M $LiPF_6$ in TMS 10 wt.% VC, the cathode is covered with small aggregates (Fig. 2d). This 'micro-roughness' may indicate the formation of an SEI layer.

The discharge capacity of the $LiMn_2O_4$|PE3|Li cell depends on the current rates (Fig. 4). The highest capacity (ca. 138 mAh g^{-1}) was obtained at the lowest rate, C/10. The cell could operate relatively efficiently, over many cycles, at higher rates. The discharging rate C/5 led to an electrode capacity of ca. 100 mAh g^{-1}. However, at the rate C/2, the discharge capacity dropped to 80 mAh g^{-1}. The same pattern was observed for charging capacity. The charge capacity was much higher than discharge capacity in the case of the current rates C/7 (ca. 150 mAh g^{-1}) and C/10 (ca. 160 mAh g^{-1}). A possible reason for the improvement in rate capability performance using the TiO_2-SiO_2 separator is that it can hold

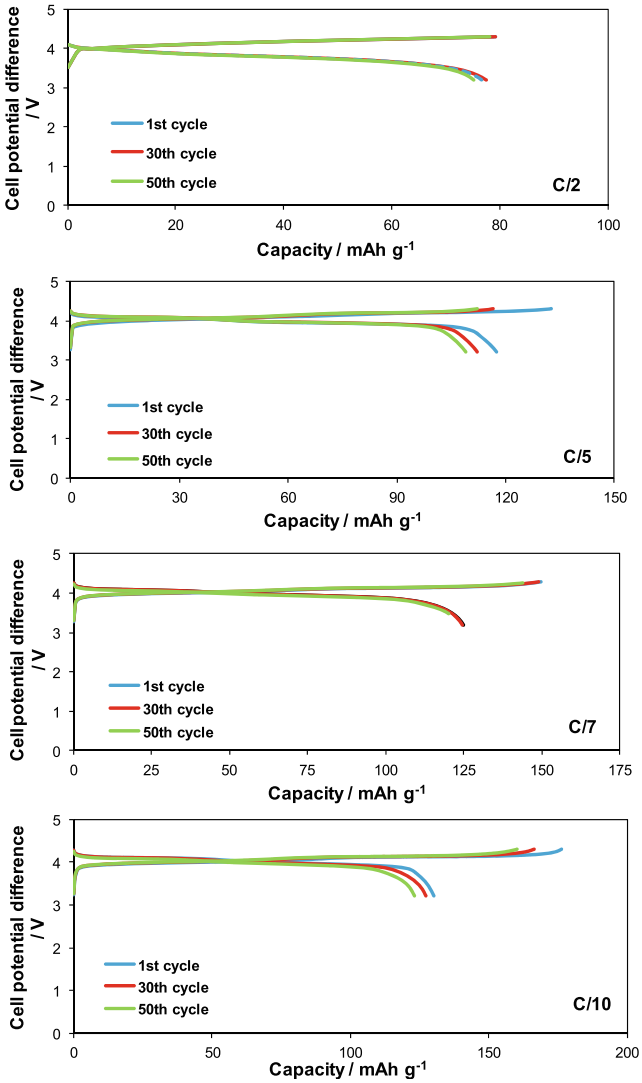

Fig. 3 Galvanostatic charging and discharging of $LiMn_2O_4$|PE3|Li system (1st, 30th, 50th cycles) at C/2, C/5, C/7 and C/10 rates

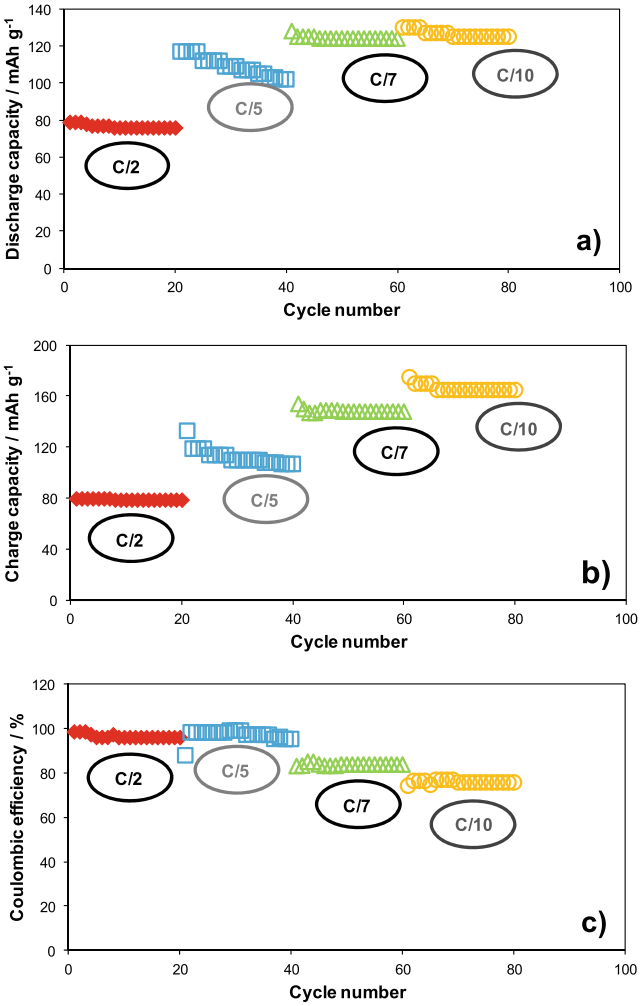

Fig. 4 Discharge capacity (**a**), charge capacity (**b**) and coulombic efficiency (**c**) of $LiMn_2O_4$|PE3|Li cell of different C rates

enough electrolyte to satisfy the demand of Li-ion rapid transmission [57]. Hence, we observed a decrease in coulombic efficiency to 85 % (C/7) and 78 % (C/10).

For comparison, the cells using the polymer separator and the SiO_2 separator exhibited initial discharge capacities of 101.95 and 108.46 mAh g^{-1}, respectively. The cell with the SiO_2 separator always has higher discharge capacity and much better cycling performance than that with the polymer separator. After 50 cycles, the discharge capacities of the cells with the polymer separator and the SiO_2 separator were 89.63 and 101.45 mAh g^{-1}, respectively. The capacity retention of the cell with the SiO_2 separator (91.6 %) is higher than that for the polymer separator (87.93 %). A possible reason for the improvement in the cell cycling performance is reduced side reactions, since SiO_2 can capture the trace amounts of moisture and acidic impurity in the electrolyte to reduce the formation and growth of the SEI film [57].

Figure 5 shows how the capacitance of the $LiMn_2O_4$|PE3|G cell depends on the number of cycles. The charging capacity of the $LiMn_2O_4$/G cell was ca. 240 mAh g^{-1} after the first cycle and stabilized at about 182 mAh g^{-1} after 100 cycles. During cycling at 25 °C, the cell lost 0.02 % of its capacity per cycle.

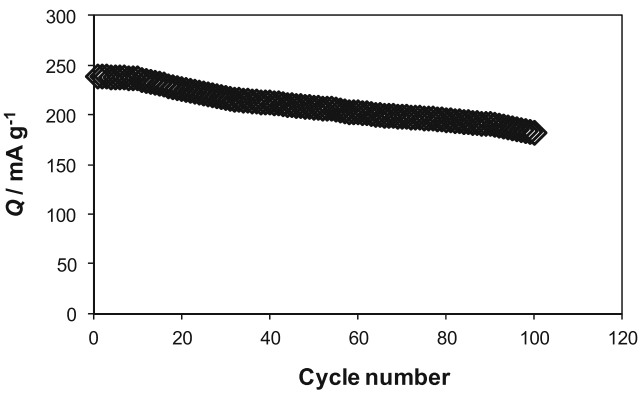

Fig. 5 Charge capacity of the $LiMn_2O_4$|PE3|G. Current rate C/5

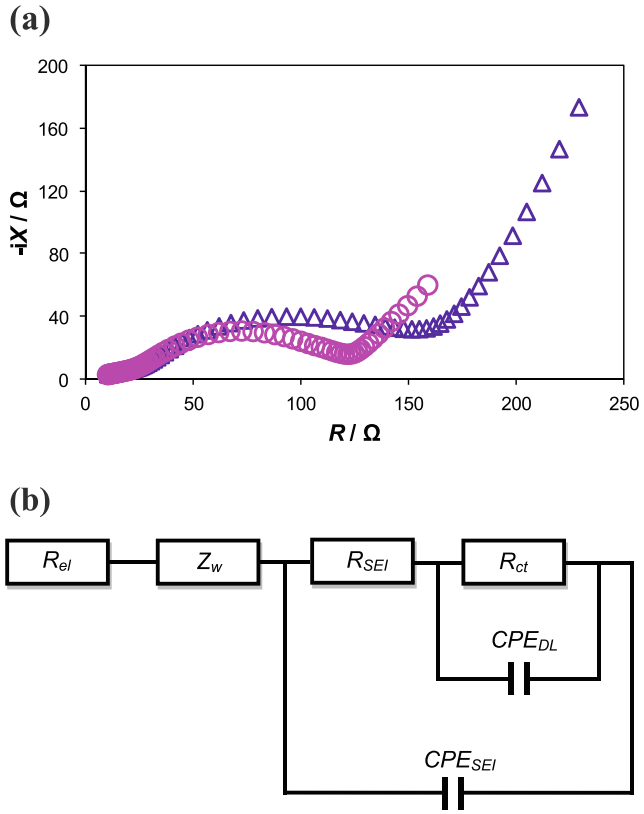

Fig. 6 Impedance spectra of the $LiMn_2O_4$|PE3|Li system taken immediately after cell assembling (*white triangle*) and after galvanostatic charging/discharging (*white circle*) (**a**) and an equivalent circuit representing the electrode/electrolyte system (**b**)

Figure 6 shows impedance spectra for the $LiMn_2O_4$|PE3|Li system taken immediately after the assembly of the cell and after galvanostatic charging/discharging. In the case of all salts, the impedance of the system decreased after electrochemical SEI formation. The impedance of the initial system (without galvanostatic polarisation) may be interpreted as being the result of the reaction of lithium with the electrolyte (solvent and salt) with the formation of a passivation layer. This system has the highest impedance (of the order of 125 Ω per 1 cm^2 of the lithium's geometrical surface area). During the electrochemical charging/discharging, the passivation layer is modified as a result of changes in thickness, composition (solid lithium salts and polymers) and morphology.

As a result of the lithium/electrolyte interphase modification, the total resistance (impedance) also changes. In the case of $LiMn_2O_4$|PE3|Li, the total impedance increases by ca. 20 %. This may suggest that, in the case of Li|($LiPF_6$ in TMS), the specific morphology (particles rather than a film layer) is due to the formation of solid particles of Li salt (for example LiF) surrounded by a polymer film [58–61].

The EIS curves for the $LiMn_2O_4$ electrode covered with the SEI layer are shown in Fig. 6a (after intercalation and after 40 galvanostatic charging/discharging cycles). The curves consist of a 'flat semicircle' or two semicircles at higher frequencies and a line at lower frequencies. The shape of the flat semicircle is a result of a combination of at least two time constants *RC*, due to the SEI layer (R_{SEI}, C_{SEI}) and due to the charge transfer process occurring at the double layer formed between the SEI and the electrodes (R_{ct}, C_{dl}). The incline line in the low frequency is associated with Li-ion diffusion in the $LiFePO_4$ particles and represents the Warburg impedance (Z_W). The equivalent circuit used for impedance spectra deconvolution is shown in Fig. 6b. In the case of the $LiMn_2O_4$|PE3|Li system, low impedance values were observed (Fig. 6a). After 40 galvanostatic charging/discharging cycles, the charge transfer resistance and SEI resistance were 62 Ω and ca. 100 Ω, respectively. The large value of SEI resistance indicates that the protective layer has a different structure than in the case of graphite. There are two possible reasons for the increase in impedance: (1) a chemical reaction at the electrode surface may cause the SEI to increase in thickness upon cycling; (2) the crystalline structure of the $LiMn_2O_4$ cathode material may be changed substantially during cycling.

The capacitance of both SEI (C_{SEI}) and the double layer (C_{dl}) is of the order of 10^{-6} F. The impedance Z_W is mainly due to lithium diffusion between graphene layers and in the $LiMn_2O_4$ particles. The R_{ct} value should be regarded as the sum of the charge transfer resistance and Warburg impedance ($R_{ct}+Z_W$). This is due to the diffusion of lithium within a solid electrode. Of course, the slow diffusion of lithium in the solid electrodes (graphite, the cathode) is the stage limiting the rate of the charge transfer process, which results in high resistance.

Conclusions

A new type of filler for gel polymer electrolytes has been used in a $LiMn_2O_4$|PE3|Li cell. We have described some of the structural properties and preliminary electrochemical results for both unmodified and modified hybrid TiO_2-SiO_2 ceramic powders. During the emulsion-precipitation process, the particle size as well as morphology can be monitored. Moreover, the obtained filler exhibits better affinity to the polymer matrix. New ceramic fillers greatly facilitate solvent uptake by dry PAN/TMS with $LiPF_6$ membranes, but only if they have been surface-modified.

Good ionic conductivity (9.8×10^{-4} and 1.5×10^{-3} S cm^{-1} at 25 and 60 °C, respectively) and the fast method of preparation show the CPE to be a suitable electrolyte for application in flexible lithium-ion batteries. Charge-discharge tests of a $LiMn_2O_4$|PE3|Li cell at different C rates reveal good specific capacities of 120 and 160 mAh g^{-1} at C/5 and C/10, respectively. All of the results obtained show that the $LiMn_2O_4$|PE3|Li cell is a good candidate for use in lithium-ion batteries.

Hybrid TiO_2-SiO_2 powders can be regarded as promising filler materials for composite polymer-ceramic gel electrolytes used in Li-ion batteries.

Acknowledgments This work was supported by Polish National Centre of Science research grant no. 2011/01/B/ST8/03961(TJ) and Poznan University of Technology research grant: 03/31/DSMK/0284 (BK).

References

1. Meyer WH (1998) Polymer electrolytes for lithium-ion batteries. Adv Mater 10:439–448
2. Tarascon JM, Armand M (2001) Review article issues and challenges facing rechargeable lithium batteries. Nature 414:359–367
3. Tang CY, Hackenberg K, Fu Q, Ajayan PM, Ardebili H (2012) High Ion Conducting Polymer nanocomposite electrolytes using hybrid nanofillers. Nano Lett 12:1152–1156
4. Ju SH, Lee Y-S, Sun Y-K, Kim D-W (2013) Unique core-shell structured $SiO_2(Li^+)$ nanoparticles for high-performance composite polymer electrolytes. J Mater Chem 395-401
5. Kim SH, Choi KH, Cho SJ, Kil EH, Lee SY (2013) Mechanically compliant and lithium dendrite growth-suppressing composite polymer electrolytes for flexible lithium-ion batteries. J Mater Chem 4949-4955
6. Lee YS, Ju SH, Kim JH, Hwang SS, Choi JM, Sun YK, Kim H, Scrosati B, Kim DW (2012) Composite gel polymer electrolytes containing core-shell structured $SiO_2(Li^+)$ particles for lithium-ion polymer batteries. Electrochem Commun 17:18–21
7. Kim KM, Park NG, Ryu KS, Chang SH (2006) Characteristics of PVdF-HFP/TiO_2 composite membrane electrolytes prepared by phase inversion and conventional casting methods. Electrochim Acta 51:5636–5644
8. Cao J, Wang L, He XM, Fang M, Gao J, Li JJ, Deng LF, Chen H, Tian GY, Wang JL, Fan SS (2013) In situ prepared nano-crystalline TiO_2–poly(methylmethacrylate) hybrid enhanced composite polymer electrolyte for Li-ion batteries. J Mater Chem 5955-5961
9. Noto VD, Lavina S, Giffin GA, Negro E, Scrosati B (2011) Polymer electrolytes: Present, past and future. Electrochim Acta 57:4–13
10. Cao J, Wang L, Shang Y, Fang M, Deng L, Gao J, Li J, Chen H, He X (2013) Dispersibility of nano-TiO_2 on performance of composite polymer electrolytes for Li-ion batteries. Electrochim Acta 111: 674–679
11. Chhabra V, Pillai V, Mishra BK, Morrone A, Shah DO (1995) Synthesis, Characterization, and properties of microemulsion-mediated nanophase TiO_2 particles. Langmuir 11:3307–3311
12. Li B, Wang X, Yan M, Li L (2003) Preparation and characterization of nano-TiO_2 powder. Mater Chem Phys 78:184–188
13. Chen YF, Lee CY, Yeng MY, Chiu HT (2003) Preparing titanium oxide with various morphologies. Mater Chem Phys 81:39–44
14. Eiden-Assmann S, Widoniak J, Maret G (2004) Synthesis and characterization of porous and nonporous monodisperse colloidal TiO_2 particles. Chem Mater 16:6–11
15. Bonne M, Pronier S, Can F, Courtois X, Valange S, Tatibouet J-M, Royer S, Marecot P, Duprez D (2010) Synthesis and characterization of high surface area TiO_2/SiO_2 mesostructured nanocomposite. Solid State Sci 12:1002–1012
16. Siwinska-Stefanska K, Ciesielczyk F, Kolodziejczak-Radzimska A, Paukszta D, Sójka-Ledakowicz J, Jesionowski T (2012) TiO_2-SiO_2 inorganic barrier composites: from synthesis to application. Pigm ResinTechnol 41:139–148
17. Malwadkar SS, Gholap RS, Awate SV, Korake PV, Chaskar MG, Gupta NM (2009) Physico-chemical, photo-catalytic and O_2-adsorption properties of TiO_2 nanotubes coated with gold nanoparticles. J Photochem Photobiol A 203:24–31
18. Kanna M, Wongnawa S (2008) Mixed amorphous and nanocrystalline TiO_2 powders prepared by sol-gel method: Characterization and photocatalytic study. Mater Chem Phys 110:166–175
19. Karuppuchamy S, Iwasaki M, Minoura H (2007) Physico-chemical, photoelectrochemical and photocatalytic properties of electrodeposited nanocrystalline titanium dioxide thin films. Vacuum 81:708–712
20. Chaimberg M, Cohen Y (1990) Note on the silylation of inorganic oxide supports. J Colloid Interface Sci 134:576–579
21. Iijima M, Kobayakawa M, Kamiya H (2009) Tuning the stability of TiO_2 nanoparticles in various solvents by mixed silane alkoxides. J Colloid Interface Sci 337:61–645
22. Bhaumik A, Tatsumi T (2000) Organically modified titanium-rich Ti-MCM-41, Efficient catalysts for epoxidation reactions. J Catal 189: 31–39
23. Bhaumik A, Tatsumi T (2000) Double organic modification by 3-chloropropyl and methyl groups on pure silica MCM-41 and Ti-MCM-41: efficient catalyst for epoxidation of cyclododecene. Catal Lett 66:181–184
24. Siwinska-Stefanska K, Ciesielczyk F, Nowacka M, Jesionowski T (2012) Influence of selected alkoxysilanes on dispersive properties and surface chemistry of titanium dioxide and TiO_2–SiO_2 composite material J Nanometer art. no. 316173 doi: 10.1155/2012/316173
25. Nilchi A, Janitabar-Darzi S, Mahjoub AR, Rasouli-Garmarodi S (2010) New TiO_2/SiO_2 nanocomposites – Phase transformations and photocatalytic studies. Colloids Surf A Physicochem Eng Asp 361:25–30
26. Zhan S, Chen D, Jiao X (2007) Mesoporous TiO_2/SiO_2 composite nanofibers with selective photocatalytic properties. Chem Commun 20:2043–2045
27. Nowacka M, Siwińska-Stefańska K, Jesionowski T (2013) Dispersive evaluation and surface chemistry of advanced, multifunctional silica/lignin hybrid biomaterials. Colloid Polym Sci 291: 1860–1873
28. Song JY, Wang YY, Wan CC (1999) Review of gel-type polymer electrolytes for lithium-ion batteries. J Power Sources 77:183–197
29. Stephan AM, Kumar SG, Renganathan NG, Kulandainathan MA (2005) Characterization of poly(vinylidene fluoride–hexafluoropropylene) (PVdF–HFP) electrolytes complexed with different lithium salts. Eur Polym J 41:15–21
30. Jacob M, Hackett E, Giannelis EP (2003) From nanocomposite to nanogel polymer electrolytes. J Mater Chem 13:1–5
31. Agrawal RC, Pandey GP (2008) Solid polymer electrolytes: materials designing and all-solid-state battery applications: an overview. J Phys D Appl Phys 41:0022–3741
32. Jeon BH, Yeon JH, Kim KM, Chung IJ (2002) Preparation and electrochemical properties of lithium-sulfur polymer batteries. J Power Sources 109:89–97
33. Wang J, Liu L, Ling Z, Yang J, Wan C, Jiang C (2003) Polymer lithium cells with sulfur composites as cathode materials. Electrochim Acta 48:1861–1867
34. Jeon BH, Yeon JH, Chung IJ (2003) Preparation and electrical properties of lithium–sulfur-composite polymer batteries. J Mater Process Technol 143–144:93–97
35. He X, Shi Q, Zhou X, Wan C, Jiang C (2005) In situ composite of nano SiO_2–P(VDF-HFP) porous polymer electrolytes for Li-ion batteries. Electrochim Acta 51:1069–1076
36. Ryu HS, Ahn HJ, Kim KW, Ahn JH, Lee JY, Cairns EJ (2005) Self-discharge of lithium–sulfur cells using stainless-steel current-collectors. J Power Sources 140:365–369
37. Jeong SS, Lim YT, Choi YJ, Cho GB, Kim KW, Ahn HJ, Cho KK (2007) Electrochemical properties of lithium sulfur cells using PEO polymer electrolytes prepared under three different mixing conditions. J Power Sources 174:745–750
38. Hassoun J, Sun YK, Scrosati B (2011) Rechargeable lithium sulfide electrode for a polymer tin/sulfur lithium-ion Battery. J Power Sources 196:343–348
39. Hassoun J, Scrosati B (2010) Moving to a Solid-State Configuration: A valid approach to making lithium-sulfur batteries viable for practical applications. Adv Mater 22:5198–5201

40. Jin J, Wen Z, Liang X, Cui Y, Wu X (2012) Gel polymer electrolyte with ionic liquid for high performance lithium sulfur battery. Solid State Ionics 225:604–607
41. Jeddi K, Ghaznavi M, Chen P (2013) A novel polymer electrolyte to improve the cycle life of high performance lithium–sulfur batteries. J Mater Chem A1:2769–2772
42. Gabrisch H, Ozawa Y, Yazami R (2006) Crystal structure studies of thermally aged $LiCoO_2$ and $LiMn_2O_4$ cathodes. Electrochim Acta 52:1499–1506
43. Zhang SS, Jow TR (2002) Optimization of synthesis condition and electrode fabrication for spinel $LiMn_2O_4$ cathode. J Power Sources 109:172–177
44. Xia Y, Yoshio M (1997) Studies on Li-Mn-O spinel system (obtained from melt-impregnation method) as a cathode for 4 V lithium batteries Part IV. High and low temperature performance of $LiMn_2O_4$ J Power Sources 66:129–133
45. Zheng H, Zhang H, Fu Y, Abe T, Ogumi Z (2005) Temperature effects on the electrochemical behavior of spinel $LiMn_2O_4$ in quaternary ammonium-based ionic liquid electrolyte. J Phys Chem B 109: 13676–13684
46. Zheng H, Li B, Fu Y, Abe T, Ogumi Z (2006) Compatibility of quaternary ammonium-based ionic liquid electrolytes with electrodes in lithium ion batteries. Electrochim Acta 52:1556–1562
47. Lalia BS, Yoshimoto N, Egashira M, Morita M (2010) A mixture of triethylphosphate and ethylene carbonate as a safe additive for ionic liquid-based electrolytes of lithium ion batteries. J Power Sources 195:7426–7431
48. Egashira M, Kanetomo A, Yoshimoto N, Morita M (2010) Electrode properties in mixed imidazolium ionic liquid electrolytes. Electrochem 78:370–374
49. Wu B, Pei F, Wu Y, Mao R, Ai X, Yang H, Cao Y (2013) An electrochemically compatible and flame-retardant electrolyte additive for safe lithium ion batteries. J Power Sources 227:106–110
50. Swiderska-Mocek A (2014) Properties of $LiMn_2O_4$ cathode in electrolyte based on ionic liquid with and without gamma-butyrolactone. J Solid State Electrochem 18:1077–1085
51. Kurc B (2014) Gel electrolytes based on poly(acrylonitrile)/sulpholane with hybrid TiO_2/SiO_2 filler for advanced lithium polymer batteries. Electrochim Acta 125:415–420
52. Akashi H, Shibuya M, Orui K, Shibamoto G, Sekai K (2002) Practical performances of Li-ion polymer batteries with $LiNi_{0.8}Co_{0.2}O_2$, MCMB, and PAN-based gel electrolyte. J Power Sources 112:77–582
53. Lewandowski A, Swiderska-Mocek A, Waliszewski L (2013) Li^+ conducting polymer electrolyte based on ionic liquid for lithium and lithium-ion batteries. Electrochim Acta 92:404–411
54. Xiang HF, Yin B, Wang H, Lin HW, Ge XW, Xie S, Chen CH (2010) Improving electrochemical properties of room temperature ionic liquid (RTIL) based electrolyte for Li-ion batteries. Electrochim Acta 55:5204–5209
55. Sakaebe H, Matsumoto H (2003) N-Methyl-N-propylpiperidinium bis(trifluoromethanesulfonyl)imide (PP13–TFSI) – novel electrolyte base for Li battery. Electrochem Commun 22:594–598
56. Reiter J, Nadherna M (2012) N-Allyl-N-methylpiperidinium bis(trifluoromethanesulfonyl) imide – A film forming ionic liquid for graphite anode of Li-ion batteries. Electrochim Acta 71:22–26
57. Chen J, Wang S, Cai D, Wang H (2014) Porous SiO_2 as a separator to improve the electrochemical performance of spinel $LiMn_2O_4$ cathode. J Membr Sci 449:169–175
58. Aurbach D (2000) Review of selected electrode–solution interactions which determine the performance of Li and Li ion batteries. J Power Sources 89:206–218
59. Chen L, Wang K, Xie X, Xie J (2007) Effect of vinylene carbonate (VC) as electrolyte additive on electrochemical performance of Si film anode for lithium ion batteries. J Power Sources 174:538–543
60. Buqa H, Golob P, Winter M, Besenhard JO (2001) Modified carbons for improved anodes in lithium ion cells. J Power Sources 97–98: 122–125
61. Andersson AM, Edström KJ (2001) Chemical composition and morphology of the elevated temperature SEI on graphite. Electrochem Soc 148:A1100–A1109